# Design and Feasibility Tests of a Gas-driven Bionic Flytrap Soft Robot

**Jian Li**
Northeast Forestry University
**Jie Yan** ( yanjie1690@163.com )
Northeast Forestry University
**Meizhen Huang**
Northeast Forestry University
**Yangwei Wang**
Northeast Forestry University

**Original Article**

**Keywords:** Flytrap, Soft Robot, Gas-driven, Flexible bending

**Posted Date:** December 8th, 2021

**DOI:** https://doi.org/10.21203/rs.3.rs-1113013/v1

**Title page**

Design and Feasibility Tests of a Gas-driven Bionic Flytrap Soft Robot

Corresponding author：Jie Yan　E-mail：yanjie1690@163.com

ORIGINAL ARTICLE(or REVIEW)

# Design and Feasibility Tests of a Gas-driven Bionic Flytrap Soft Robot

**Jian Li[1] • Jie Yan[1] • Mei-Zhen Huang[1] • Yang-Wei Wang[1]**

**Abstract:** The research of bionic soft robot is a complex system engineering, including soft matrix material, soft actuator, soft sensor and bionic control system. Unlike most animals, plants cannot move in whole voluntarily. However, for the purpose of energy and nutrition, various parts of the plant body also carry out various movements, which vary from millisecond to hour on a large time scale. As a result, Plants are considered a source of inspiration for innovative engineering solutions, and a growing number of researchers are investigating the mechanisms of plant movement and biomimetic research. In this paper, the biological morphology, microstructure and movement mechanism of Venus flytrap leaf were studied and analyzed, and a bionic flytrap grassland machine with chamber design was designed and manufactured. Firstly, according to the research report on the biological morphology, microstructure and movement mechanism of Venus flytrap, the idea of chamber design was determined. Based on this observation, we reconstructed the leaf model and bionic structure of Venus flytrap by reverse modeling. Based on the principle of turgor pressure deformation, the chamber design rules of bionic Venus flytrap blade were formulated and optimized with silica gel as the bulk material. The flow channel design of Venus flytrap blade was studied and explored. Finally, the bionic Venus flytrap leaf was made by 3D printing technology and silica gel casting process, and the two bionic leaves were clamped at a certain opening Angle. The bending performance of bionic flytrap blade and the flytrap closure experiment were studied by air pressure excitation. The experimental results show that the bionic Venus flytrap blade can complete bending and closing experiments, and the bionic Venus flytrap can complete the whole capturing process within 5s. The leaf opening Angle of the bionic Venus flytrap reaches 80 degrees, which fits well with the real Venus flytrap blade and meets the design requirements and bionic goals. Apparently, this study is the first to design the chamber of the bionic flytrap leaf, formulate rules, and study the possibility of its deformation. It provides a new idea for the study of the movement and deformation of plant leaves, and expands the application of bionic robots, especially the robot solutions for plant types.

**Keywords:** Flytrap • Soft Robot • Gas-driven • Flexible bending

✉ YAN jie
Yanjie1690@163.com

[1] College of Mechanical and Electrical Engineering, Northeast Forestry University, Harbin 150040, China

## 1 Introduction

Soft robot technology involves new materials, new manufacturing technology and new control methods, which has become an important research direction and has been paid attention to by researchers at home and abroad. Compared with traditional rigid robots, soft robots are made of soft materials, and can be continuously deformed, greatly bending, twisting and stretching, with higher flexibility, safety and adaptability. After hundreds of millions of years of evolution, organisms have their own characteristics of motor ability and environmental adaptability. Therefore, biological soft tissue and structure have become the object of study and study for scientists in the field of soft robot, mainly including natural invertebrates or vertebrate boneless limbs, such as starfish, worms, jellyfish, octopus, elephant trunk and the tongue of mammals.[1] From the point of view of structure, the soft tissue structure of these animals mainly includes two kinds: hydrostatic skeletal structure and muscular hydrostatic skeletal structure. Hydrostatic bone structure is a closed cavity formed by muscles, which is filled with body fluid. The static pressure of the closed fluid is used to transmit force and cause body deformation and movement by

controlling the contraction of different parts of muscles. The muscular hydrostatic skeleton has no closed fluid cavity and consists entirely of muscle fibers aligned in different directions. Contraction of muscles in one direction and extension of muscles in the other direction remain constant in volume, causing deformation and movement of the body. Unlike most animals, plants cannot move in whole voluntarily. However, for the purpose of obtaining energy and nutrition, each part of the plant body also carries out various movements, including growth movement, tropism movement, perceptual movement, feeling movement and so on. Plant movements span a wide range of time scales, from milliseconds to hours. Most movements are usually slow and unnoticeable, such as climbing and winding. But the tactile movement of the leaves of insectivorous plants can catch insects that can move or even fly, such as Venus flytraps[2].

In terms of driving modes, pneumatic, hydraulic and intelligent materials (such as shape memory alloy, electric-driven polymer, dielectric elastomer, intelligent gel) and other driving modes are widely used in soft robots, among which gas driving is the research hotspot in recent years[3,4]. The research group of Professor George M. Whitesides of Harvard University has made remarkable achievements in gas-driven soft robots. By using silicon rubber as the matrix, combined with soft lithography technology, microfluidic technology and 3D printing technology, it has prepared bionic tentacles, bionic starfish and other actuators, realizing the ability of grasping and manipulating complex shapes[5,6]. The development of Octobot, a soft-bodied octopus robot driven by gas generated by chemical reactions, represents a major breakthrough in the research of soft-bodied robots. The results were also published in《Nature》[7,8]. Ecole Polytechnique Federale de Lausanne and Zhejiang University developed bionic robot fish driven by dielectric high projectile body respectively[9]. Deakin University, Australia, combined with 3D printing technology, prepared a polyelectrolyte software driver using porous chitosan[10]. The University of Science and Technology of China (USTC) has developed a radio-symmetric soft robot driven by shape memory alloy, which can move well in water and sand[11]. Researchers from Italy and Shanghai Jiao Tong University have developed a rope driven soft silicone arm that mimics the tentacles of octopuses, respectively, and is capable of flexibly grasping objects[12]. Shenyang Institute of Automation, Chinese Academy of Sciences has developed a bionic fish with liquid crystal film driven by ultraviolet light by the phase transformation reaction of azobenzene chromophore under light[13]. The IpMC-powered bionic jellyfish robot was developed at Virginia Tech[14]. Tongji University proposed a new self-actuated bionic soft robot manipulator based on ionic gel. The above driving methods have their own advantages and disadvantages: the overall flexibility of the pneumatic mechanism is the best, but the rigidity is insufficient, need compressor and other auxiliary devices; Shape memory wires most closely resemble muscle performance, but are limited in frequency; Rope drive itself does not have the output of force and displacement, requiring additional drive elements; Dielectric elastomer drive voltage is high, difficult to use; The output force of IPMC and intelligent gel materials is small[15-18].

In the field of locomotion and biomimetic research, Brazilian scientists have studied how plants conduct mechanical stimuli and trigger movement at the molecular level[19]. The University of Washington has analyzed and summarized three types of power sources for plant motion: osmosis, colloid based drive, and fibre-based drive, in order to broaden the interest of researchers in plant mimicry[20]. Harvard University has studied the mechanics of the capillary or complex fluid involved in plant movement[21]. Tohoku University in Japan has studied the chemical mechanisms that open and close the leaves of nocturnal plants. On the basis of studying the motion mechanism of plants, bionic mechanism also began to appear. Lanzhou University and Xi 'an Jiaotong University have studied the magnetically driven petal-like flexible gripper[22]. Italian scientists have developed a tendril soft robot based on ion electroadsorption on a flexible porous carbon electrode[23]. A team at Finland's Tampere University of Technology created a light-driven artificial Venus flytrap based on light-responsive liquid crystal elastomers. The results of the two bionic plant robots are published in《Nature Communications》[24].

In this paper, we seek a bionic Venus flytrap based on Venus flytrap. Firstly, the biological morphology and movement mechanism of Venus flytrap were studied, and then the key structural parameters of Venus flytrap leaf were obtained by reverse modeling the leaf with 3D scanner. Then, the chamber design rules of the flytrap blade were formulated, and the optimization design and flow channel design were carried out. Finally, 3d printing technology and silica gel casting process were used to fabricate the bionic flytrap leaf with silica gel as the body material. The experimental results show that the bionic flytrap blade can complete the bending and closing experiments and meet the design requirements. Therefore, the biomimetic Venus flytrap software robot developed in this paper has important reference value for the study and

application of plant biomimetic and living capture.

## 2 Flytrap - Inspired Soft Robot

### 2.1 Biological Characteristics of Flytrap

*2.1.1 Biological Morphology of Flytrap*

Venus flytrap, a perennial herb native to North America, is a very interesting insectivorous plant. Its stem very short, at the top of the leaf has a insect resembling a "shell" clip, and can secrete juices. When bug broke into, flytrap and translate at breakneck speed clamp, and digestion and absorption.

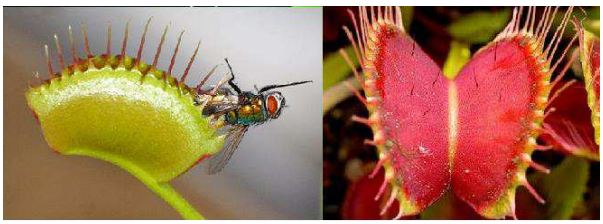

**Figure 1** The integral morphology of Venus flytrap

As shown in Fig. 1, Venus flytraps have complete roots, stems, leaves, flowers, and seeds. Its blade is the main and most obvious place, has the function of the insects, visible sting and red sessile glands, looks like a tooth claw maw. The Venus flytrap has regular bristles along the edges of the leaves, and secretory glands at the base of the bristles secrete mucus to prevent the insect from breaking away and sticking to the petals.

**Figure 2** Leaf morphology of Venus flytrap

For the leaf of Venus flytrap, the veins of Venus flytrap leaf were obtained after transparent treatment. As shown in Fig. 2, it can be clearly seen that the leaf vein structure of Venus flytrap has obvious hierarchical characteristics, and the main axial veins are regularly distributed in a fan shape. The lateral veins divide the leaf into several chambers of different sizes, forming a network pattern. The lumen size of the leaf blade is outside near the bristles, becoming denser and finer. Bristles are spaced at the tip of leaf blade. The top and bottom of the whole blade present an elliptic curve. The blade presents an outward-convex state when it is not closed, and an inward-concave state when it is closed.

*2.1.2 The Development Mechanism of Curl Deformation in the Leaves of Flytrap*

Venus flytraps capture insects through four steps: luring them, trapping them, breaking them down and absorbing them, and sustaining their growth. Venus flytraps are extremely complex, with symmetrical leaves connected by petioles. Venus flytraps attract insects by producing nectar from nectaries along the edges of their leaves. When the insect is attracted to land on the leaf, the leaf will close quickly when the insect touches the trigger villi in the trap twice within a certain period of time, transmitting a signal. There are regular bristles along the edge of the leaf, which are arranged in a staggered pattern when the leaf is closed, forming a cage from which the insect cannot escape. And there is a slime system at the bottom of the bristles, which can stick to the insects and prevent them from escaping. The insect is then digested and absorbed, using the nutrients to sustain the Venus flytrap's own growth.

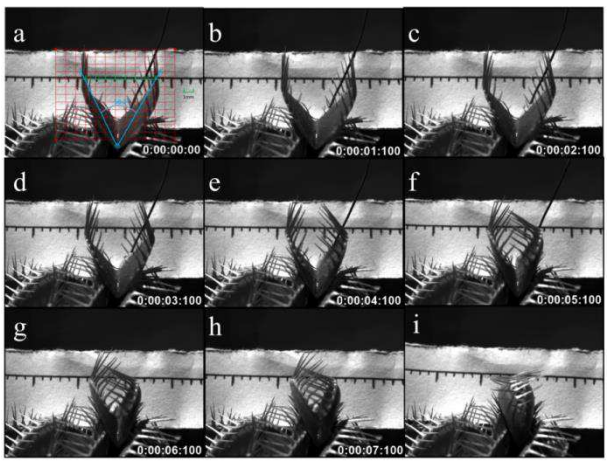


**Figure 3** Venus flytrap capture process

Flytrap action mechanism: fly initial condition for the lateral bending in leaf, when inside the trigger villi feel mechanical stimulation, electrical signals can cause the directional movement of the ions in the organization, form of chemical potential difference, and lead to the flow of water, under the action of water pressure, cause the slow deformation of wall of a cell, and store the elastic potential energy, the curvature of the leaf blade flattened gradually; When water pressure reaches a critical threshold, under the action of geometric constraints, elastic potential energy of

ontology sudden release translates into kinetic energy, blade quickly buckling, realize the change of curvature from convex to concave, caused by passive flow can provide the viscous resistance to balance the elasticity, constant pressure supply makes the blade in a necked-in condition.

Generally, the whole movement of Venus flytraps can be divided into three stages: initial stage, capture stage and digestion stage. In the initial stage of Venus flytrap, the two leaves are open and symmetrically distributed. Figure 3 shows the initial stage of Venus flytrap. In the initial state, the leaf opening Angle of Venus flytrap is 58.2 degrees, and the top spacing of leaves is 7.7mm. In the capture stage, when the Venus flytrap is stimulated twice within a certain time interval, the leaves close quickly to complete the capture action. Figure 1 (a - h) as the Venus flytrap capture stage, in the capture phase, flytrap can in 4 to 6 seconds to complete the closing of the leaf (wild flytrap time will be shorter, the fastest can be completed in 0.5 seconds to capture action), sting mutual crisscross, prevention and treatment of prey escape, fly at this time of grass piece is not closed completely, but entered the stage of digestion. During the digestion phase, the flytrap leaf slowly closes until the prey is digested and absorbed.

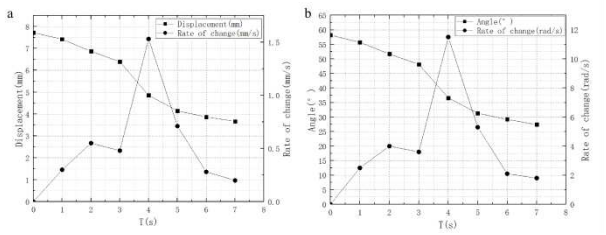


**Figure 4** Quantitative analysis of flytrap movement process

At various stages of the process of the Venus flytrap movement on quantitative analysis of figure 4 to fly top in leaf spacing and distance change rate and the relation curve of time, we found that the fly can be done in 4 to 5 seconds in leaf blade fold movement, showed a trend of decreasing the top spacing, distance change rate present a parabolic trend, top at 0 to 4 seconds, The top spacing of Venus flytrap decreased and the change rate increased. At the fourth second, the change rate of top space of Venus flytrap reached the peak, which was 1.53mm/s. At 4-7 seconds, the change rate of the top spacing of Venus flytrap showed a decreasing trend and gradually entered a gentle stage. At this time, the top spacing was 3.67mm, and the spines of Venus flytrap interlaced with each other. The catching stage of Venus flytrap ended and it entered the digestion stage. Until the end of the digestion phase, fly the top spacing in leaf, tend to be 0. Figure 4 to fly open in leaf Angle and Angle change rate and the relation curve of time, we found the Venus flytrap during the initial phase of the blade open Angle of 58.2 degrees, the capture phase, the blade open Angle decreases, when reduced to 27 degrees or so, the Angle of the blade changes to flatten out. The Angle change rate of the leaf of the Venus flytrap presented a parabolic trend. From 0 to 4 seconds, the Angle of the leaf of Venus flytrap gradually decreased, and the Angle change rate gradually increased, and reached the peak at 4 seconds. At this time, the Angle of the leaf of Venus flytrap was 36.6 degrees, and the Angle change rate was 11.5rad/s. After 4 seconds, the leaf Angle of the Venus flytrap continued to decrease, and the Angle change rate gradually decreased. After the capture stage, the Angle change rate tended to be gentle, and the Angle gradually decreased, and the Venus Flytrap entered the digestion stage.

Based on the above analysis, during the capture stage of Venus flytrap, the top spacing and Angle of Venus flytrap leaf gradually decreased, and the corresponding change rate presented a parabolic trend, which reached the peak value in 4 seconds, and then gradually slowed down, and entered the digestion stage in 7 seconds. At the digestion stage, the top spacing and Angle of the Venus flytrap gradually decrease until the top spacing and Angle change to zero. At this time, the Venus flytrap blade will remain for a period of time (Fig.3-i) until the prey is digested, and then the leaf will open and enter the next capture stage.

## 2.2 Structural Design of Bionic Leaf

### *2.2.1 Rules for Chamber Design of Bionic Leaf and Establishment of Three Dimensional Model of Bionic Leaf*

When conducting bionic research on Venus flytrap, the structural size of Venus flytrap blade is needed first. As shown in Fig. 5， the appropriate leaf of Venus flytrap was selected, and the leaf point cloud data of Venus flytrap was obtained by 3D scanning of Venus flytrap leaf. Then the point cloud data of leaves are processed and screened. Get quality point cloud data. The 3d leaf model of Venus flytrap was obtained by reverse modeling the leaf with point cloud data. Extract the flytrap leaf surface, key size measurement was carried out on the blade surface, get fly in leaf size parameters of the 2d. Proper adjustment of parameters, to get fly in leaf size parameters of the 2d. Because the flytrap ontology in leaf size is small, is not conducive to simulation and post-production, so to catch flies in leaf five times for the 2d dimension parameters of the amplifier, enlarged size parameters of the blade. At this point, the maximum transverse size of the blade is 120mm, and the bottom size is 90mm. B-spline curve is used to fit the

curves at the top and bottom of the blade, and circles R=10 and R=5 are respectively used for transition processing at the junction between the curve and the radial straight line. At this point, the Venus flytrap leaf size and leaf two-dimensional model has been established.

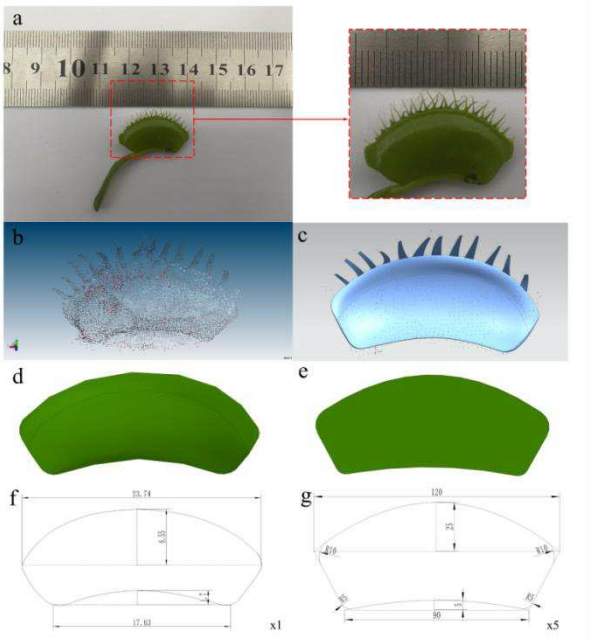


**Figure 5** The key dimensions of flytrap leaf were obtained

After the two-dimensional dimension parameters of the flytrap leaf were obtained, the leaf mesh was divided. As shown in Fig. 6, the chamber division rules of Venus flytrap leaves are shown. The thick solid black line is the boundary curve of the flytrap leaf, the solid blue line is the inner boundary curve of the flytrap leaf, the dotted black line is the invalid grid line, the dotted green line is the effective grid line, the solid green line is the outdoor boundary of the effective cavity, the fine solid black line is the indoor boundary of the effective cavity, and the dotted red line is the center line. The rules are as follows: for a Venus flytrap leaf, use d1 to establish the inner boundary of the leaf. Starting from the apex of the upper boundary of the inner boundary of the flytrap blade, draw a radial line with d3 as the ruler, and starting from the center line, draw a horizontal line with d2 as the ruler, so as to obtain the leaf grid division scheme with d1, d2 and d3 as the ruler. The effective grid area (green dotted line area) after partition was selected, and d4 was taken as the chamber thickness to obtain the cavity division scheme of blades.

In this paper, a Gas-driven bionic flytrap is studied. The blade is mainly composed of deformation layer and constraint layer. Its working principle is to realize the bending deformation of the blade by taking advantage of the great difference in ductility between deformation layer and constraint layer and the asymmetry of silicone rubber matrix structure. As shown in Fig.6, green is the deformation layer and gray is the constraint layer, where the deformation is composed of the chamber layer and the sealing layer. Among them, T1 is the limiting layer, T2 is the chamber layer, and T3 is the sealing layer. At this point, the structural parameters of the flytrap leaf are obtained as shown in Table 1, and the three-dimensional model of the bionic flytrap leaf is established.

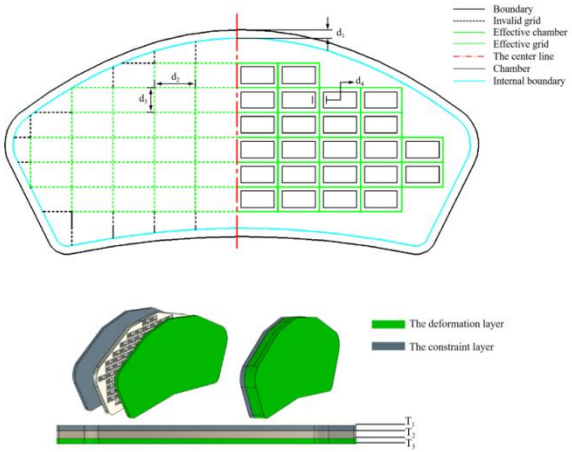


**Figure 6** The key dimensions of flytrap leaf were obtained

**Table 1** The structural dimensions of the flytrap leaf mm

| Name | Implication | Name | Implication |
|---|---|---|---|
| d1 | Inner boundary distance | T1 | Deformation layer thickness |
| d2 | Radial distance | T2 | Chamber layer thickness |
| d3 | Axial distance | T3 | Sealing layer thickness |
| d4 | Chamber thickness | | |

### *2.2.2 Deformation Mechanism of Bionic Leaf*

Silicone rubber material has good scalability and fracture elongation can reach 800%. Therefore, silicone rubber is selected as the material for the preparation of bionic Venus flytrap leaves. For the study of nonlinear mechanical model of hyperelastic material, considering the isotropy and incompressibility of hyperelastic material, silica gel with Shore hardness of 20 is selected as the main material of the soft driver. Because the strain energy density function of Yeoh model has outstanding advantages in describing the large deformation of hyperelastic materials, this paper adopts the Yeoh model to establish the constitutive model of silicone rubber materials, and determines the material parameters of Yeoh as the material parameters of finite element simulation combined with tensile test.

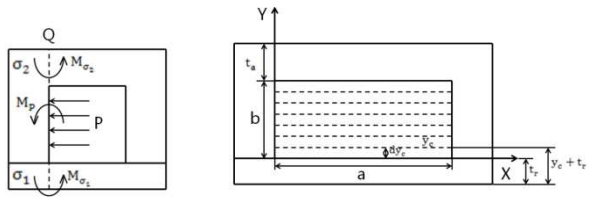


**Figure 7** A single chamber stress analysis

The general strain energy density function of the Yeoh model can be expressed as:

$$W = W(I_1, I_2, I_3) = \sum_{i=1}^{N} C_{i0}(I_1 - 3)^i + \sum_{k=1}^{N} \frac{1}{d_k}(J-1)^{2k} \tag{1}$$

In the function (1):

$$\begin{cases} I_1 = \lambda_1^2 + \lambda_2^2 + \lambda_3^2 \\ I_2 = \lambda_1^2\lambda_2^2 + \lambda_2^2\lambda_3^2 + \lambda_1^2\lambda_3^2 \\ I_3 = (\lambda_1\lambda_2\lambda_3)^2 \end{cases} \tag{2}$$

In the formula(1), $I_{1,2,3}$ are deformation tensor invariants, $N$、$C_{i0}$ and $d_k$ are material parameters, $\lambda_1$, $\lambda_2$ and $\lambda_3$ are form variables in three directions in space, where $\lambda_1$ is the main stretch ratio in the elongation direction, and $\lambda_2$ and $\lambda_3$ are the secondary stretch ratio in the other directions. $J = I_3 = 1$ for incompressible hyperelastic materials, so the general strain energy density function expression of Yeoh model can be simplified into two expansions of typical strain energy density function:

$$W = C_{10}(I_1 - 3) + C_{20}(I_1 - 3)^2 \tag{3}$$

In the formula(3), $C_{10}$ and $C_{20}$ are steady-state coefficients of silicone rubber material based on Yeoh model, and their values can be measured by uniaxial tensile test. According to the tensile test and the actual deformation of the tensile test specimen, the material parameters of silicone rubber based on the Yeoh model can be obtained as $C_{10} = 0.14$ and $C_{20} = 0.00086$.

According to this paper studies the pneumatic bionic flytrap structure characteristics in leaf, when a series of Chambers arranged in a certain rule, filling the gas because of the asymmetry of the structure and deformation layer and limits of the difference of ductility can cause blade towards limiting layer on one side of the bend, the assumptions in the process of bending layer bottom length $I_0$ remains the same, and blade chamber to produce steady deformation, Finally, a uniform arc with a bending radius of $R_d$ and a bending Angle will be generated($\varphi$). Since the air pressure of each chamber is the same when the blade is deformed, a single chamber is selected for force analysis in order to establish the mechanical model when the blade is bent and deformed and carry out force analysis. As shown in FIG. 3, the gas chamber is expanded and deformed, and the driving bending moment generated at the inner wall ($Q$) in the air chamber is $M_p$.The top of the deformed layer and the bottom portion of the restriction layer bending with the cavity deformation, the resistance torque generated by the inner silicone interior ($Q$) of the cavity bottom restriction layer silica gel is $M_{\sigma 1}$.The resistance torque generated by the internal stress ($Q$) between the upper silica gel of the deformation layer gas chamber is $M_{\sigma 2}$. By the torque balance available:

$$M_p = M_{\sigma 1} + M_{\sigma 2} \tag{4}$$

As shown in Fig. 7, the inner wall of the cavity is divided into a small rectangular region having a large length $a$ and width $dy_c$. The area of each small rectangle is $ady_c$, and the gas pressure is $aPdy_c$. The distance between the gas chamber and the restriction layer bottom point (O) is $y_c + t_r$.Gas pressure torque generated by the small rectangle is $aP(y_c + t_r)dy_c$ .The torque $M_p$ produced by the gas pressure on the inner wall of the gas chamber is the sum of the torque generated by the gas pressure of each small rectangle. The torque $M_p$ can be expressed as:

$$M_P = aP\int_0^b (y_c + t_r)dy_c = aP(b^2 + 2t_r b) \tag{5}$$

In the formula(5), $a$ is the length of the air cavity, $t_r$ is the limiting layer silicone thickness, and $p$ is the drive input gas pressure. Simultaneously, the torque $M_{\sigma 1}$ generated by the restriction layer section stress, the torque $M_{\sigma 2}$ generated by the cross-sectional stress of the deformation layer is:

$$M_{\sigma_1} = \sigma\int_0^{t_r} (a + 2t_a)y_r dy_r = \frac{\sigma {t_r}^2 (a + 2t_a)}{2} \tag{6}$$

$$M_{\sigma_2} = \sigma\int_0^{b+t_a} a(y_c + t_r)dy_c - \sigma\int_0^b (a + 2t_a)(y_c + t_r)dy_c = \frac{\sigma(2abt_a + a{t_a}^2 - 2b^2 t_a + at_a t_r - 2bt_a t_r)}{2} \tag{7}$$

In the formula(6) and (7), $t_a$ is a deformable layer silica gel thickness, $\sigma$ is a section tensile stress. It can be seen from the above in the above formula, to obtain torque $M_{\sigma 1}$ and $M_{\sigma 2}$ need to determine the value of stress $\sigma$ . The literature can be seen that the tensile stress is:

$$\sigma = 8C_{10}(\lambda_1 - 1) \tag{8}$$

In the formula(8), $\lambda_1$ is the principal elongation ratio. $\lambda_1$ can be expressed as:

$$\lambda_1 = \frac{I}{I_0} \tag{9}$$

In the formula(9), $I$ and $I_0$ are the length of the chamber bending and the initial length, respectively.. The bending length $I$ and the bend angle $\phi$ have the following relationship:

$$\frac{1}{\pi R_d} = \frac{\phi}{180} \tag{10}$$

In the formula(10), $R_d$ is a bending radius. Therefore, the relationship between the form of the chamber bending angle and the air pressure can be obtained:

$$\phi = \phi\ (P) \tag{11}$$

$$\phi = \frac{180 I_0}{\pi R_d}\left[\frac{2a(b_2 + 2bt_r)}{8C_{10}\left(2abt_a + a{t_r}^2 + a{t_a}^2 + 2t_a{t_r}^2 - 2b^2 t_a + at_a t_r - 2bt_a t_r\right)}P + 1\right] \tag{12}$$

It can be seen from the above formula, the bending angle of the blade is related to the input pressure $P$ , the cavity length $a$ , the gas chamber thickness $b$ , the restriction layer silicone thickness $t_r$ , the deformed layer silicone thickness $t_a$ , the blade initial length $I_0$ , and the bending radii $R_d$ . Coupled deformation occurs between the chambers and the chambers by controlling whether each chamber of the blade is inflated. The coupling deformation of the blade under different chamber layout is obtained by simulation and experiment.

*2.2.3 Optimization of Structural Parameters of Three-Dimensional Model of Bionic Leaf*

In this chapter, the structural parameters of Venus flytrap blades are analyzed and optimized. Using orthogonal test and range analysis method, seven structural parameters of the leaf of Venus flytrap were taken as the influencing factors, and two dimensional bending angles of the leaf of Venus flytrap were taken as the response index. The effects of seven structural parameters on the bending deformation of flytrap blades in two dimensions were studied through simulation analysis. Finally, the optimization design was carried out to maximize the bending Angle of two dimensions, and the optimal combination of structural parameters was selected. Table 2 is the level table of orthogonal test factors of flytrap leaves. Seven structural parameters of the flytrap leaf were selected as the study factors, and five levels were selected for each factor.

**Table 2** Orthogonal test factors and levels

| No. | d1 | d2 | d3 | d4 | T1 | T2 | T3 |
|---|---|---|---|---|---|---|---|
| 1 | 0.5 | 4 | 4 | 0.5 | 1 | 1 | 1 |
| 2 | 1 | 6 | 6 | 1 | 2 | 2 | 2 |
| 3 | 1.5 | 8 | 8 | 1.5 | 3 | 3 | 3 |
| 4 | 2 | 10 | 10 | 2 | 4 | 4 | 4 |
| 5 | 2.5 | 12 | 12 | 2.5 | 5 | 5 | 5 |

The leaf of bionic Venus flytrap was simulated and analyzed by ABAQUS software to study the deformation under 0.3kpa pressure excitation. The bending angles of two dimensions are obtained by data extraction from simulation results. Significance analysis was performed on the data.The model significance difference level is P=0.028, and the regression equation relationship is significant. R2a=0.764 and R2b=0.632, indicating that the regression is effective and the experimental results are reliable. It can also be seen from Table 3 that d3、T1 and T3 have a significant impact on the in-plane bending Angle of x-Y of bionic biological Venus flytrap leaves.d1、d4、T1 and T3 had a great influence on the x-z in-plane bending Angle of the bionic Flytrap leaf.Through orthogonal test, we obtained the optimal parameter combination of bionic flytrap leaf: d1 =0.5mm, d2 =8mm, d3 =6mm, d4 =0.5mm, T1 =1mm, T2 =2mm, T3 =1mm.Considering the influence of the manufacturing process, the size of the chamber will be limited to a certain extent. Therefore, the structural parameters of the bionic Flytrap blade are set as d1 =2mm, d2 =10mm, d3 =6mm, d4 =1mm, T1 =2mm, T2 =2mm, T3 =2mm.Simulation results are obtained through simulation analysis as shown in Fig. 8. x-y in-plane bending Angle of the bionic Flytrap blade is 38°, and x-z is 18°.

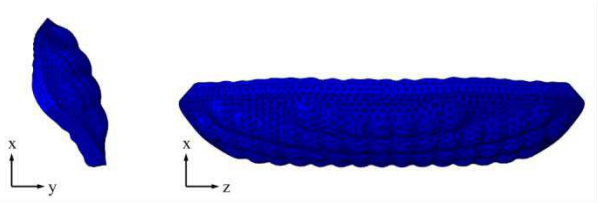


**Figure 8** Simulation result

## 3 Flow Channel Design and Result Analysis of Bionic Leaf

In the second chapter, we optimize the structural parameters of the bionic flytrap blade, and obtain the optimal parameter combination of the bionic flytrap blade. In the chamber design of the Venus flytrap leaf, the ratio of D2 to D3 has a certain influence on the shape of the chamber, and the chamber size is limited due to the development of the manufacturing process. Therefore, taking the above factors into consideration, this chapter will conduct flow channel design for the three structural parameters of the flytrap blade, and explore how the bending situation of the bionic Flytrap blade in two dimensions will be affected when the flow channel scheme is changed.

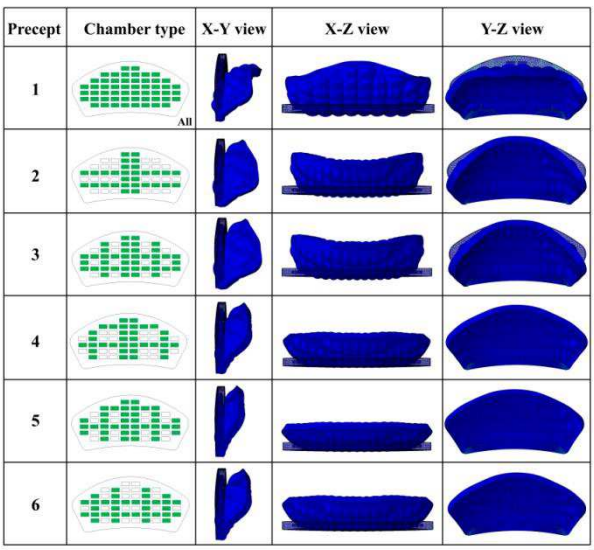


**Figure 9** d2＞d3

As shown in Fig. 9, is the chamber layout when d2 is larger than d3. On this basis, the flow channel design is carried out. In order to make the bionic Flytrap blade bend in two dimensions and have a certain enveloping property, the flow channel layout is designed in transverse and longitudinal directions. In Fig. 9, 6 flow channel design schemes are listed. Precept 1 is the deformation of the

chamber when it is fully inflated. At this time, the in-plane bending Angle of X-Y is 36.75 degrees, and the in-plane bending Angle of X-Z is 26.67 degrees. Precept 2-6 is a flow channel scheme designed with certain rules. By comparison, we can clearly find that: The bending angles of Precept 2-6 are all smaller than that of Precept 1, and deformation coordination exists. For example, in Precept 2 and Precept 3, the bending of the middle part of the blade is obviously weaker than that of the two sides of the blade, indicating that in the chamber layout when d2 is larger than d3, the deformation is the best when all the air is filled.

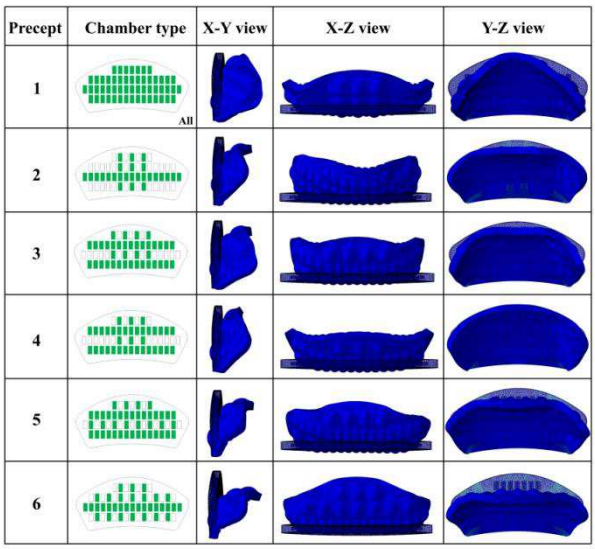


**Figure 10** d2＜d3

As shown in Fig. 10, is the chamber layout when d2 is less than d3, and the flow channel design is carried out similarly. Among the 6 Precept listed, Scheme 1 is the deformation under the condition that the chamber is fully inflated. At this time, the in-plane bending Angle of X-Y is 26.39 degrees, and the in-plane bending Angle of X-Z is 24.54 degrees, and the deformation is not coordinated. Precept 2-6 is a flow channel scheme designed with certain rules. By comparison, we can clearly find that: The deflection of the 6 best, and the deformation coordination is the best, at this point the x-y in-plane bending Angle of 50.73 degrees, x, z in-plane bending Angle of 25.57 degrees, and the air chamber compared with Precept 1, chamber amount decreased by 37%, x-y in-plane bending Angle is increased by 92%, x, z in-plane bending Angle is increased by nearly 5%.

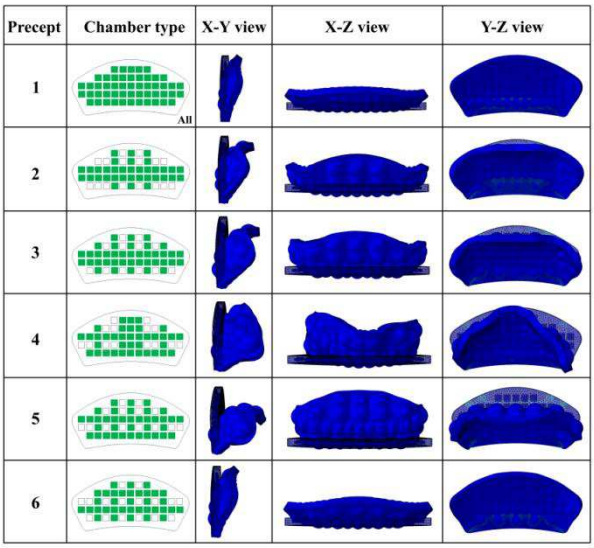


**Figure 11** d2=d3

As shown in Fig. 11, is the chamber layout when d2 is equal to d3, and the flow channel design is carried out similarly. Among the 6 schemes listed, Precept 1 is the deformation under the condition that the chamber is fully inflated, and the in-plane bending Angle of X-Y is 13.6 degrees and that of X-Z is 12.78 degrees. Precept 2-6 flow scheme of design is a certain rule, through the comparison we can clearly found that the scheme the deflection of the five best, and the deformation coordination is the best, at this point the x-y in-plane bending Angle of 51.83 degrees, x, z in-plane bending Angle of 38.3 degrees; Compared with Precept 1, the number of ventilation chambers decreased by 28%, the in-plane bending Angle of X-Y increased by 281%, and the in-plane bending Angle of X-Z increased by nearly 200%.

Through the comparison of several flow channel design schemes, it is found that different deformation can be achieved by changing the flow channel schemes under the same pressure and the same chamber layout. By contrast, found in d2 is equal to d3, the deflection of the Precept 5 and coordination meets the design requirements of bionic flytrap and deformation requirement.

## 4 Fabrication and Feasibility Tests of Bionic Flytrap Leaf

### 4.1 Fabrication of Bionic Flytrap Leaf

Silica gel casting method is mainly used to make the bionic Venus flytrap leaf. The mold required for pouring is produced by 3D printing technology. The prepared silica gel material is poured into the mold, and the silica gel is solidified and demoulded. Then the two parts of the bionic Venus flytrap leaf are combined and bonded to obtain the

bionic Venus flytrap leaf body. As shown in Fig.12, a and b are 3d printed bionic flytrap leaf casting molds. After mixing silicone rubber in a certain proportion, vacuum pump is used to remove bubbles generated in the mixing process of silicone rubber. Then the silica gel is poured into the mold. In the pouring process, due to the poor fluidity and slow flow of silica gel, the mold is slowly and evenly poured from one side during pouring. When the height of silica gel is slightly higher than the mold, the pouring is stopped. After the silica gel is poured, the deformation layer (a2) and limiting layer (b2) of the blade are obtained by standing for 4-6 hours at room temperature. For the pouring of the limiting layer, before pouring, the gauze with the same size as the blade is cut and placed in the mold of the limiting layer, and then it is poured. Then, the two parts were combined and bonded by silica gel to obtain the bionic Venus flytrap leaf body (c).

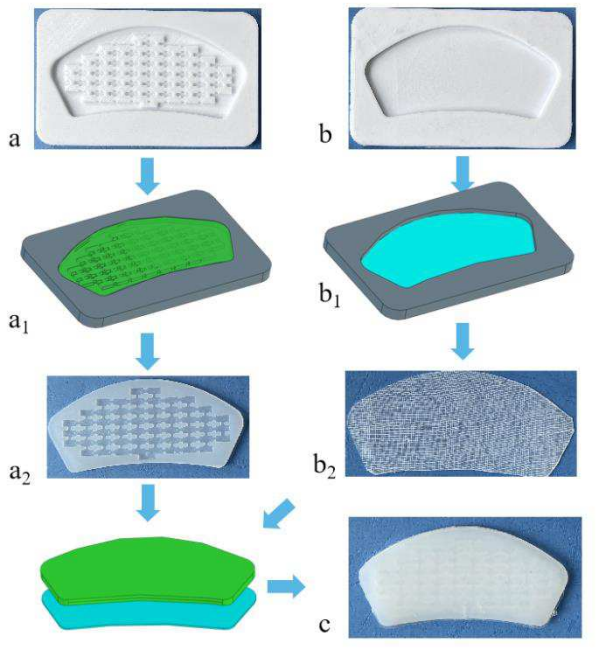


**Figure 12** Fabrication of Bionic Flytrap Leaf

### 4.2 Feasibility Tests of Bionic Flytrap Leaf

The bionic flytrap leaf is driven by gas, and the general gas is used as an incentive to drive the silicone material to deform, which can be reused for many times. After the bionic Venus flytrap leaf body was obtained by silica gel casting, the feasibility experiment was carried out. The air pump is driven by power supply, and the air pump is connected with the air pressure valve, which is connected with the blade body. By adjusting the output power of air pump and the size of air pressure valve, stable air pressure excitation can be provided for blade body.

As shown in Fig.13, we conducted experiments on the bionic flytrap leaf and compared the simulation results. Through experiments, we can know that the bionic flytrap blade designed by chamber design can complete the bending deformation of two dimensions, and the blade model made has a high degree of consistency with the simulation results. However, there are also problems of asymmetrical and uncoordinated deformation caused by uneven casting thickness of blades. In the experiment, the leaf of the bionic flytrap reaches steady-state deformation under a certain pressure excitation. At this time, the deformation of the two dimensions is basically the same as the simulation results. During the experiment, the steady-state deformation of the leaf can be changed by changing the input pressure. Under the pressure of 0.4kpa, the x-Y plane bending Angle of the blade reaches 38° and the x-Z plane bending Angle of the blade reaches 18° in the steady state. The response time of bionic flytrap leaf can be controlled by controlling the flow and velocity. Because of the different flow channel design of the bionic flytrap blade, the response time of the blade is also different under the same flow and velocity. For the bionic target, the response time of the bionic Venus flytrap blade should be as short as possible. However, considering the instability and rupture of the blade in the process of deformation, the response deformation time should be controlled within 4s by adjusting the parameters.

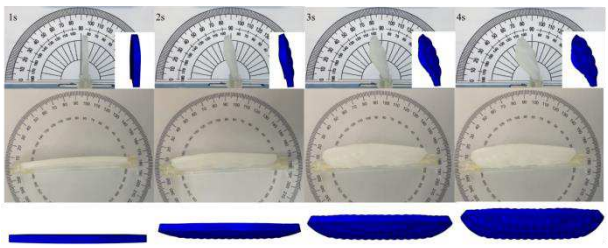

**Figure 13** Feasibility Tests of Bionic Flytrap Leaf

### 4.3 Experimental Study on Bending and Closing of Flytrap - Inspired Soft Robot

A stable air pressure excitation is provided to the flytrap leaf through an air pump and a pneumatic valve, as shown in Fig. 14. In the initial state, the bionic flytrap blade was clamped at a certain opening Angle through the fixture, and the opening Angle of the blade in this experiment was 80° . When the air source is opened, the blade deforms rapidly under pressure excitation, and the bending deformation is completed within 4s. And the blade ends begin to contact. By comparing the process in the flytrap-Inspired Soft Robot catching stage,the Flytrap-inspired Soft Robot can complete bending and closing, and has a high degree of fit

with the Flytrap deformation process. After power is switched off, Flytrap-Inspired Soft Robot is able to instantly return to its original state at room temperature. Bending closure can be repeated, and Flytrap-Inspired Soft Robot Soft Robot from bending deformation to the initial state, the whole experiment process lasts about 5s.

In the experimental process, we also found some problems, because the blade clamping is not accurate and the blade thickness error in the production will lead to the dislocation and synchronization of the two blades in the bending deformation; And because the bionic fly edge in leaf is have certain radian, so there is a edge sealing is not good, can adjust the blade by raising the pressure and open Angle that blade extrusion to improve the sealing contact, but can be by optimization to improve the sealing chamber on the edge of the blade design.

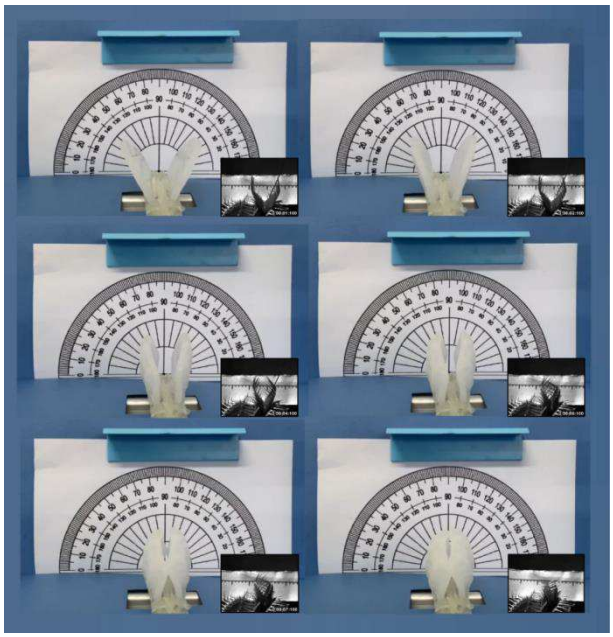

**Figure 14** Experimental Study on Bending and Closing of Flytrap - Inspired Soft Robot

## 5 Conclusions

In this paper, the biomimetic design principle is used to study the deformation characteristics of the biological form of Venus flytrap, and the biomimetic design elements are combined with the biomimetic prototype of Venus flytrap. First of all, the bionic flytrap capture stage blade deformation and microstructure of blade cell is introduced into the bionic software in the design of the innovation of the blade, through reverse modeling extraction model of blade size, design and develop a set of chamber design, the structure of bionic blade size optimization design was carried out, the chamber of the optimized layout of port design scheme, The blade with certain performance is obtained. A new type of bionic flytrap leaf blade and bionic flytrap grassland machine were developed by 3D printing technology and silica gel casting method. A series of experiments were carried out to study the bending performance of blades, and the results were compared with the simulation results. Finally, the bending and closing experiments of the bionic Venus flytrap were carried out. The experimental results show that the bionic flytrap blade can bend and close the experiment, meeting the original design requirements.

In this work, the design and manufacture of a bionic soft robot inspired by Venus flytrap is preliminarily completed. The research results are expected to provide reference value for multi-dimensional deformation applications of bionic flexible actuators. In this process, there are still some problems that need to be further studied and discussed, such as further improving the tightness of the bionic blade when it is closed, the disharmony of the blade deformation, and adding inducer and sensor to realize the function of Venus flytrap more completely. In the future, we will try to divide the blade into regions. When it is close to the blade edge, the chamber size of the blade decreases regularly to achieve more coordinated deformation at the blade edge and further improve the airtightness of the blade when it is closed. In addition, in the design of the bionic Venus flytrap system, we will try to add the micromotion sensor and the corresponding induction device, so as to obtain a more perfect and functional bionic Venus flytrap device.

## 6 Declaration

**Acknowledgements**

The authors sincerely thanks to Professor Jian Li of Northeast Forestry University for his critical discussion and reading during manuscript preparation.

**Funding**

Supported by National Natural Science Foundation of China (Grant No. 51905084)

**Availability of data and materials**

The datasets supporting the conclusions of this article are included within the article.

**Authors' contributions**

The author' contributions are as follows: LI jian and YAN jie was in charge of the whole trial; YAN jie and HUANG meizhen wrote the manuscript; WANG yangwei

and YAN jie assisted with sampling and laboratory analyses.

**Competing interests**

The authors declare no competing financial interests.

**Consent for publication**

Not applicable

**Ethics approval and consent to participate**

Not applicable

## References


[1] Forterre Y. Slow, fast and furious: understanding the physics of plant movements[J]. Journal of experimental botany, 2013, 64(15): 4745-4760.

[2] Stahlberg R. The phytomimetic potential of three types of hydration motors that drive nastic plant movements[J]. Mechanics of Materials, 2009, 41(10): 1162-1171.

[3] Fumiya Iida a, Cecilia Laschi. Soft Robotics: Challenges and Perspectives. Procedia Computer Science，2011，7 ：99-102.

[4] Rolf Pfeifer, Max Lungarella, Fumiya Iida. Soft materials may enable the automation of tasks beyond the capacities of current robotic technology. Communications Of The Acm，2012，55（11）：76-87.

[5] FilipIlievski, Aaron D. Mazzeo, Robert F. Shepherd, Xin Chen, and George M. Whitesides. Soft Robotics for Chemists.Angew. Chem. Int. Ed.，2011，50：1890-1895.

[6] Ramses V. Martinez, Jamie L. Branch, Carina R. Fish, Lihua Jin, Robert F. Shepherd, Rui M. D. Nunes, ZhigangSuo, and George M. Whitesides. Robotic Tentacles with Three-Dimensional Mobility Based on Flexible Elastomers. Adv. Mater.，2012，1-8.

[7] Michael Wehner, Ryan L. Truby, Daniel J. Fitzgerald1, Bobak Mosadegh, George M. Whitesides，etal. An integrated design and fabrication strategy forentirely soft, autonomous robots. NATURE，2016，536：451-455.

[8] Rongjie Kang, Emanuele Guglielmino，et al. Embodiment design of soft continuum robots. Advances in Mechanical Engineering，2016，8(4) ：1-13.

[9] Jun Shintake, Vito Cacucciolo, Herbert Shea, and Dario Floreano. Soft Biomimetic Fish Robot Made of Dielectric Elastomer Actuators. SOFT ROBOTICS，2018，5（4）：466-474.

[10] Ali Zolfagharian, AkifKaynak, Sui Yang Khoo. Control-Oriented Modelling of a 3D-Printed Soft Actuator. Materials，2019，12（71）

[11] Chunshan Liu, Erbao Dong, Min Xu, Gursel Alici and JieYang. Locomotion analysis and optimization of actinomorphic robots with soft arms actuated by shape memory alloy wires. International Journal of Advanced Robotic Systems，2018：1-14.

[12] M. Cianchettia, A. Arientia, M. Follador. Design concept and validation of a robotic arm inspired by the octopus. Materials Science and Engineering C，2011，31：1230-1239.

[13] Huang C, et al. Miniaturized Swimming Soft Robot with Complex Movement Actuated and Controlled by Remote Light Signals. Sci. Rep.，2015，5：17414.

[14] Joseph Najem, Stephen A Sarles, et al. Biomimetic jellyfish-inspired underwater vehicle actuated by ionic polymer metal composite actuators. Smart Materials And Structures，2012，21：094026.

[15] Vogt DM, Becker KP, Phillips BT, GrauleMA, Rotjan RD, Shank TM, et al. Shipboard design and fabrication of custom 3D-printed soft robotic manipulators for the investigation of delicate deep-sea organisms. PLoS ONE，2018，13(8)：e0200386.

[16] Kunihiko Kobayashi, ChangKyu Yoon, et al. Biodegradable Thermomagnetically Responsive Soft UntetheredGrippers. ACS Appl. Mater. Interfaces，2019，11：151−159.

[17] Brian Byunghyun Kang, Hyungmin Choi, Haemin Lee and Kyu-Jin Cho. Exo-Glove Poly II: A Polymer-Based Soft Wearable Robot for the Hand with a Tendon-Driven Actuation System. SOFT ROBOTICS，2018.

[18] Joseph D. Greer, Tania K. Morimoto, Allison M. Okamura and Elliot W. Hawkes. A Soft, Steerable Continuum Robot That Grows via Tip Extension. SOFT ROBOTICS，2018.

[19] Livia Camilla Trevisan Scorza, Marcelo Carnier Dornelas. Plants on the move: Towards common mechanisms governing mechanically-induced plant movements. Plant Signaling & Behavior，2011，6（12）：1979-1986.

[20] Jacques Dumais, Yoel Forterre. “Vegetable Dynamicks”:The Role of Water in Plant Movements. Annu. Rev. Fluid Mech，2012，44：453-478.

[21] Minoru Ueda, Yoko Nakamura. Chemical Basis of Plant Leaf Movement. Plant Cell Physiol， 2007，48(7)： 900–907.

[22] Wei Gao, Lanlan Wang§, Xingzhe Wang, and Hongzhong Liu. Magnetic Driving Flowerlike Soft Platform: Biomimetic Fabrication and External Regulation. ACS Appl. Mater. Interfaces，2016，8 (22)：14182–14189.

[23] Indrek Must, Edoardo Sinibaldi ， Barbara Mazzolai. A variable-stiffness tendril-like soft robot based on reversible osmotic actuation. Nature Communications，2019，10：344.

[24] Owies M. Wani, Hao Zeng, Arri Priimagi. A light-driven artificial flytrap. Nature Communications，2017， 8：15546.